多層微流道結構於微液滴定量與操控的應用

On-Demand Liquid-in-Liquid Droplet Metering and Fusion Utilizing Pneumatically-Actuated Membrane-Type Valves

利用薄膜快速的上下運動可將連續的水流在油流輔助下切割成微小的水滴，本研究以電腦整合眾多薄膜的運動，再配合輔助流道的設計，產生液滴定量與融合的效果，可依實際需求快速產生定量且具特定組成的液滴，並在後端整合薄膜開關以產生移動路徑切換的效果，將產生的液滴依實際需求導引至目的地。

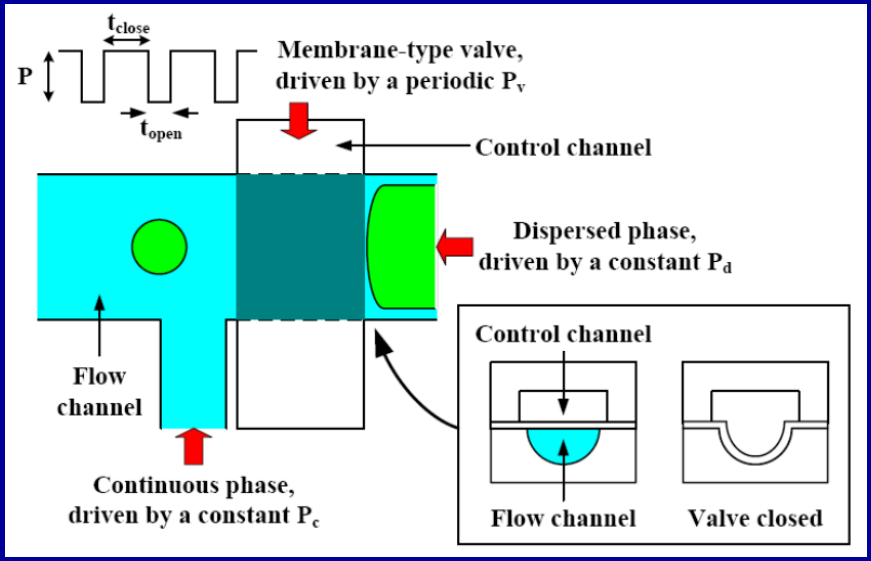

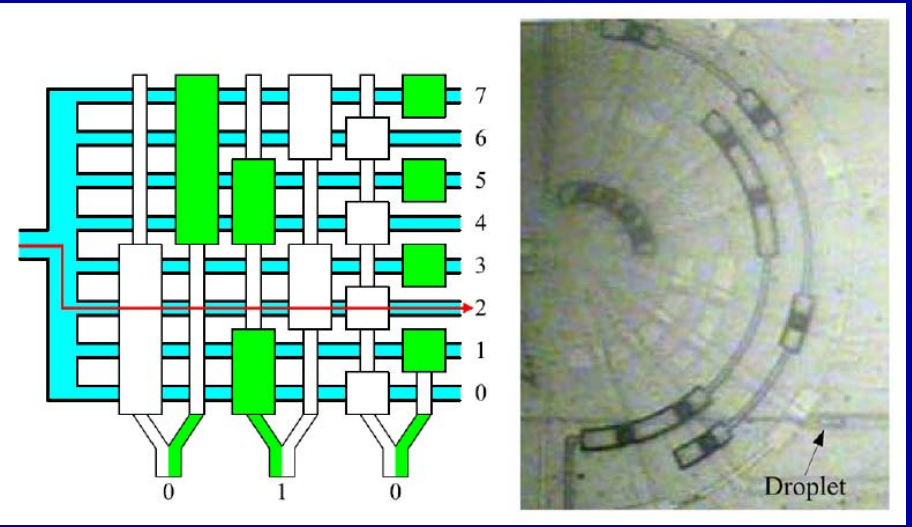

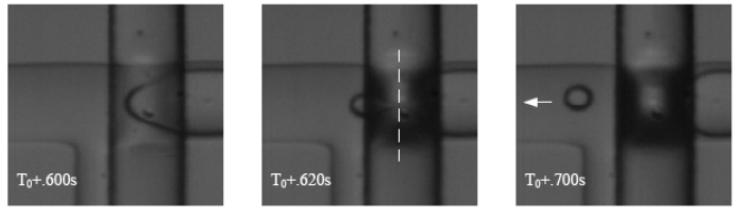

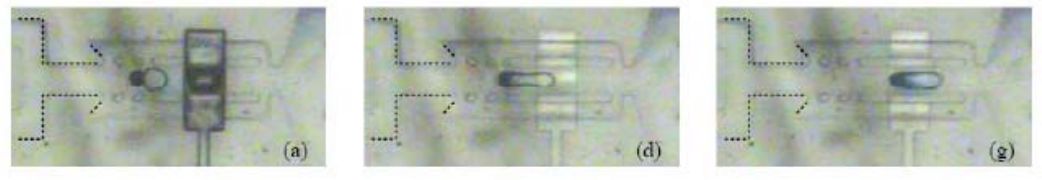

J. Micromech. Microeng. **18** (2008) 115005 (10pp) doi:10.1088/0960-1317/18/11/115005

On-demand liquid-in-liquid droplet metering and fusion utilizing pneumatically actuated membrane valves

Bo-Chih Lin and Yu-Chuan Su

Department of Engineering and System Science, National Tsing Hua University, Hsinchu, Taiwan

E-mail: ycsu@ess.nthu.edu.tw

Received 5 March 2008, in final form 28 August 2008
Published 23 September 2008
Online at stacks.iop.org/JMM/18/115005

Abstract

This paper presents an active emulsification scheme that is capable of producing micro-droplets with desired volumes and compositions on demand. Devices with pneumatically actuated membranes constructed on top of specially designed microfluidic channels are utilized to meter and fuse liquid-in-liquid droplets. By steadily pressurizing a fluid and intermittently blocking its flow, droplets with desired volumes are dispersed into another fluid. Furthermore, droplets from multiple sources are fused together to produce combined droplets with desired compositions. In the prototype demonstration, a three-layer PDMS molding and irreversible bonding process was employed to fabricate the proposed microfluidic devices. For a dispersed-phase flow that is normally blocked by a membrane valve, the relationship between the volume (V) of a metered droplet and the corresponding valve open time (T) is found to be approximately $V = kT^a$, in which k and a are constants determined mainly by the fluid-driving pressures. In addition to the metering device, functional droplet entrapment, fusion and flow-switching devices were also integrated in the system to produce desired combined droplets and deliver them to intended destinations upon request. As such, the demonstrated microfluidic system could potentially realize the controllability on droplet volume, composition and motion, which is desired for a variety of chemical and biological applications.

(Some figures in this article are in colour only in the electronic version)

Introduction

Mixing immiscible fluids together results in an emulsion, which might be defined as a heterogeneous system consisting of at least one fluid (in the form of tiny droplets) dispersed within another fluid [1]. An emulsion does not form spontaneously. It is produced by an emulsification process, through which interfaces between fluids are created and stabilized by some emulsifying agents. For example, massive production of emulsions is traditionally performed by mechanical agitation, ultrasonication or high-pressure homogenization [2–4]. However, the results of these emulsification processes are usually poorly controlled and highly polydisperse. Monodisperse emulsions are highly desirable for a variety of applications, including agriculture, the petroleum industry and pharmaceutical products [5, 6]. Recently, various microfluidic emulsification schemes such as T-junctions [7–9] and flow-focusing devices [10–12] have been demonstrated to be capable of producing emulsions in a consistent and controlled manner. In general, emulsions of micro-droplets with a $<10\%$ diameter variation can be readily produced by these approaches, and the average droplet size can be adjusted by varying the flow rates of the fluids involved in the process.

Among the various types of microfluidic systems, droplet-based systems have recently attracted significant interest because of their potential impact on diverse chemical and biological applications [13–15]. By compartmentalizing reactions into micrometer-sized droplets, the miniaturization and large-scale parallel processing of reactions, which are desired for applications involving the investigation of huge parameter spaces, could eventually be realized. The resulting

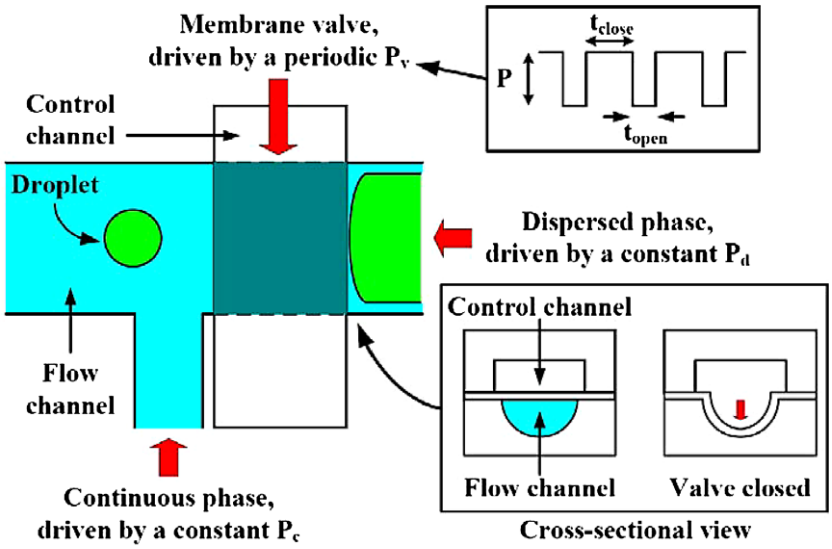

Figure 1. Schematic illustration of the proposed metering scheme.

low sample consumption and high reaction throughput are expected to significantly accelerate the progress in drug discovery, protein crystallization and various chemical and biological screening and synthesis [16–19]. Metering is the starting point and often the most critical function of a droplet-based system. In most microfluidic emulsification schemes, droplet metering is controlled by adjusting the flow rates of the dispersed and continuous phase fluids, which are driven by separate syringe pumps. In general, these passive schemes are capable of producing continuous droplet streams, but insufficient for adjusting the droplet size and breakup frequency in a real-time manner [20, 21]. The resulting droplet volume and breakup frequency are often coupled, and there is always a transition period following the adjustment of fluid flow rates. Fusion, in which droplets from multiple sources are merged together to form a desired combined droplet, is another crucial function for droplet-based systems. Previously, droplet fusion has been demonstrated by utilizing size and frequency matching [22], converging fluidic channels [23], or patterned ITO electrodes [24], which result in the deceleration and collision of droplets. However, the coordination of droplet motion is increasingly difficult, when more droplets are to be merged. Meanwhile, the employment of syringe pumps as driving sources has made it costly when trying to scale up the complexity and productivity of the systems.

To address the need for a better controllability on droplet size, composition and motion, this paper presents an active emulsification scheme that employs pneumatic actuation for the metering, fusion and manipulation of droplets. Devices with membranes constructed on top of specially designed micro-fluidic channels are utilized to realize the desired controllability. Three accomplishments have been achieved (1) a membrane-actuated metering device that can produce monodisperse droplets and adjust the droplet size and breakup frequency in a real-time manner; (2) a droplet entrapment and fusion device that can selectively and temporally block the movement of droplets, and facilitate the fusion of the entrapped droplets; and (3) an active droplet-based microfluidic system that can produce droplets with desired sizes and compositions on demand, and deliver the droplets to intended destinations upon request. As such, the demonstrated microfluidic devices could potentially realize the controllability on droplet size, composition and motion, which is desired for various chemical and biological applications.

Operating principle

A schematic illustration of the proposed metering scheme is shown in figure 1. A microfluidic device, made up of a *T*-junction with a membrane valve mounted on its top, is employed to control the emulsification process. The structure of the pneumatically driven, membrane valve is similar to a previous work [25], while a flat membrane sandwiched between the control and flow channels is utilized in our design. Whenever a sufficient pressure is applied to the upper control channel, the membrane deflects downward and blocks the lower flow channel. The dispersed and continuous phase fluids are driven independently by pressures with constant magnitudes of P_d and P_c, respectively, and fed into the corresponding microfluidic channels. Without membrane actuation, liquid-in-liquid droplets with certain dimensions can be produced at specific frequencies, and the result can be adjusted by varying the fluid-driving pressures P_d and P_c [7]. The membrane valve is located across the flow channel and right upstream of the *T*-junction. It is driven by a constant pressure P, which is sufficient to deflect the membrane and completely block the underneath flow channel, and switched on and off using an electromagnetic actuator. Periodically, the membrane valve is pneumatically enabled (or pressurized) for t_{close} and then disabled for t_{open}. Figure 2 illustrates a complete metering cycle, in which the valve is opened for 0.075 s. The color of the membrane turns dark when the membrane deflects downward. Otherwise, the membrane is transparent and the flow in the underneath channel could be clearly observed. Normally, the valve blocks the dispersed-phase flow completely, while a limited volume of the dispersed-phase

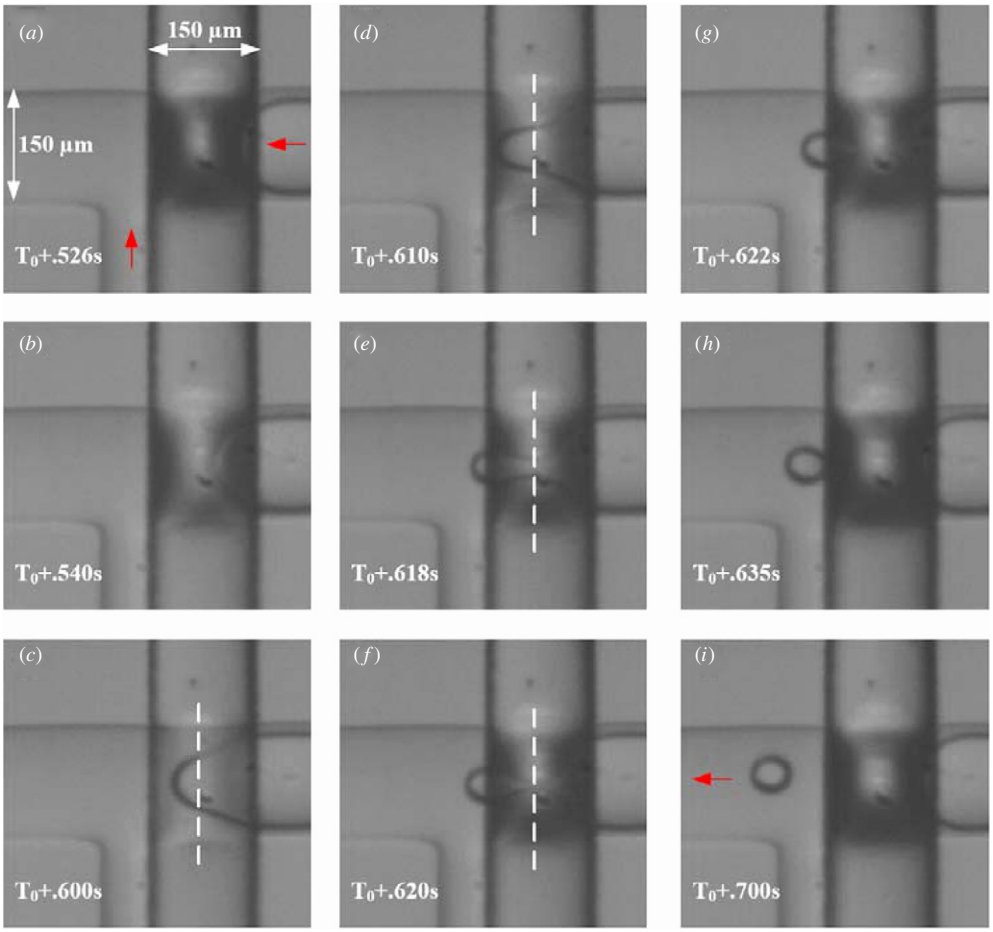

Figure 2. A complete metering cycle with $t_{open} = 0.075$ s.

fluid can flow through the path when the valve is opened. The collapse of the membrane breaks the dispersed-phase flow and produces a discrete droplet, which is then driven away from the *T*-junction by the continuous-phase flow. With the utilization of the membrane valve, the resulting droplet volume and breakup frequency could be adjusted independently by varying the open time (t_{open}) and cycle time ($t_{close} + t_{open}$) of the valve, respectively. Totally four control parameters (t_{close}, t_{open}, P_d and P_c) are utilized to regulate the metering process, so liquid-in-liquid droplets could be produced in a flexible and real-time manner. In general, the resulting breakup frequency could be either higher or lower than the original one (without valve actuation), while the resulting droplet volume would usually be smaller than what is originally achieved. The proposed metering scheme is applicable to the generation of both water-in-oil and oil-in-water droplets, when hydrophobic and hydrophilic flow channels are employed, respectively.

Once droplets (each with specific ingredient and volume) are produced, they are further fused and mixed together to produce combined droplets with desired compositions and volumes. A schematic illustration of the proposed fusion scheme is shown in figure 3. A microfluidic channel, with one end temporally blocked by a membrane valve and narrow lateral branches bypassing the incoming flow, is utilized to selectively entrap the dispersed droplets. To investigate the relevant flow behavior and facilitate the implementation of

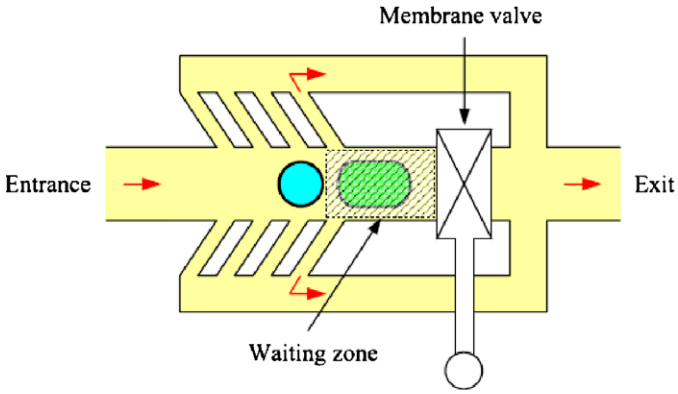

Figure 3. Schematic illustration of the proposed fusion scheme.

the proposed fusion scheme, simulation using CFD-ACE+ (CFD Research Corporation) is performed. Figure 4 shows the simulated stream lines and velocity distribution based on a simplified channel geometry. For droplets with diameters larger than half of the width of the central channel, it is expected that the droplets would be driven into the space between the valve and the last pair of the bypassing branches, while the continuous-phase fluid bypasses the blockage and keeps flowing downstream. With balanced lateral pressure,

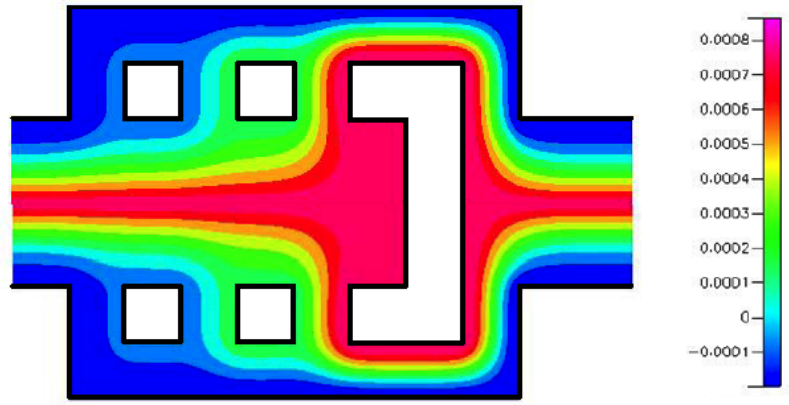

(*a*) Steam-line distribution

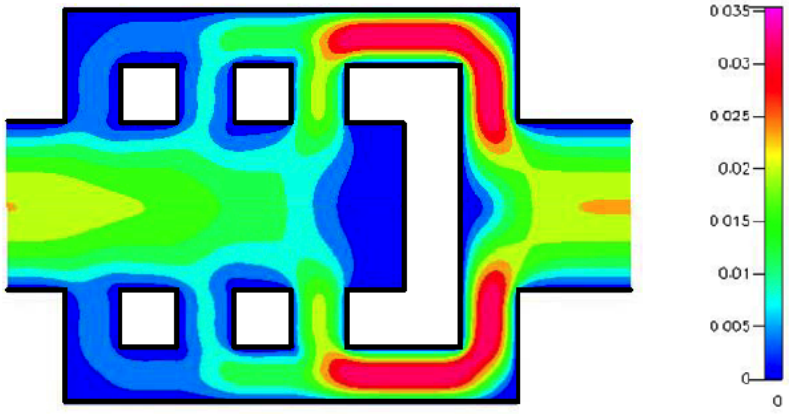

(*b*) Velocity distribution

Figure 4. Simulation results of the proposed fusion scheme.

the droplets would remain in the central portion of the main channel, slow down when moving close to the blockage, and eventually be entrapped inside the 'waiting zone', which is actually a dead volume when the channel is blocked. In the proposed fusion scheme, all the droplets to be fused would be deposited serially into the waiting zone, whose volume should be set or adjusted accordingly. With droplets restrained in the waiting zone, an incoming droplet would collide with the previously deposited ones when it arrives. Driven by the continuous-phase flow, the newly arrived droplet would push the previously deposited ones moving further into the dead end of the waiting zone, and stop when it is completely into the waiting zone. Eventually, the entrapped droplets would fuse together after a certain period of time. As such, combined droplets with desired volumes and compositions could be produced by coordinating the proposed metering and fusion schemes. Afterward, the membrane valve is opened and the combined droplet is driven downstream for further processing.

Fabrication processes

A three-layer PDMS molding and irreversible bonding process were employed to fabricate the proposed microfluidic devices, as illustrated in figure 5. First of all, a layer of 25 μm thick positive photoresist (9260, AZ Electronic Materials) was spin coated and patterned on top of a clean silicon wafer to fabricate the mold used for the duplication of the flow-channel layer. Afterward, the patterned photoresist layer was baked at 120 °C for 30 min, during which the photoresist reflowed and its profile became rounded. Meanwhile, the mold used for the duplication of control-channel layer was fabricated by coating and patterning a 10 μm thick layer of negative photoresist (SU-8, MicroChem) on top of a clean silicon wafer. After the two photoresist molds were fully cured, they were placed in a desiccator under vacuum for 3 h with a vial containing a few drops of 1H, 1H, 2H, 2H-perfluorooctyl-trichlorosilane (Fluka) to silanize the surfaces [26]. The purpose of this silanization step is to facilitate the removal of polymeric replicas (from the molds) after the following casting process. A mixture of 10:1 PDMS pre-polymer and curing agent (Sylgard 184, Dow-Corning) was stirred thoroughly and then degassed under vacuum to remove entrapped air bubbles. The casting and bonding process started with the deposition of a thin valve membrane on top of a clean silicon wafer. About one tenths of the PDMS mixture was spin coated on the wafer at 1500 rpm for 30 s, which yielded a thickness of roughly 30 μm, and cured for 15 min at 85 °C. Meanwhile, about half of the PDMS mixture was poured onto the flow-channel mold, degassed, cured for 15 min at 85 °C, and then peeled off from the mold. Afterward, the flow-channel layer was pressed and bonded on top of the 30 μm thick membrane, and

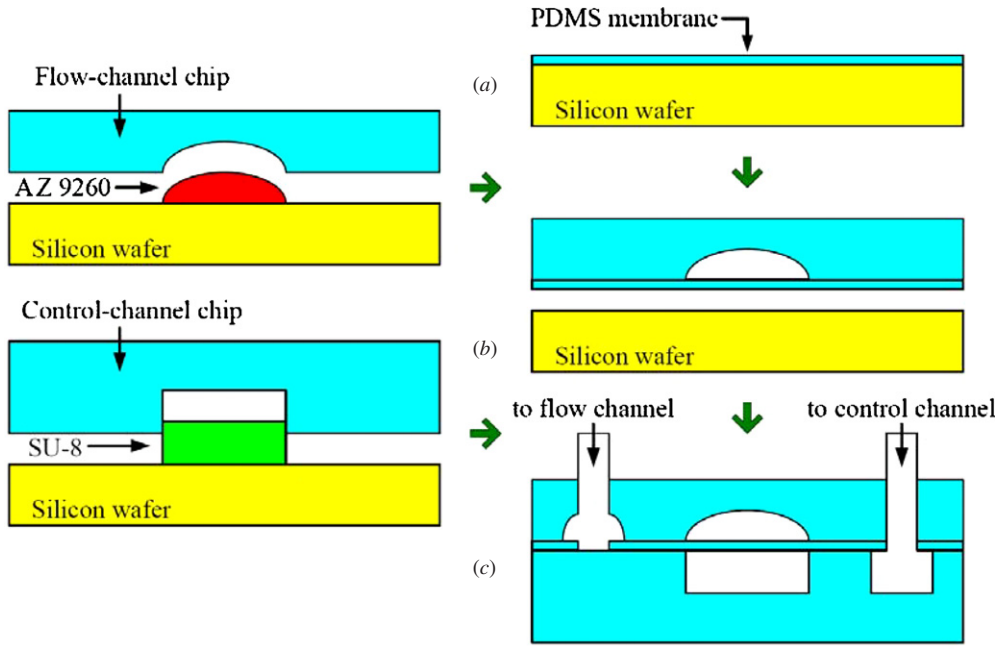

Figure 5. A three-layer PDMS molding and irreversible bonding process.

left undisturbed for at least 1 h at 85 °C for the bonding to take effect. The bonded two-layer PDMS structure was then peeled off from the silicon wafer, and punched through with a sharp metal-tube array to fabricate the holes for multiple inlets and outlets. Afterward, it was cleaned in an ultrasonic bath to remove residual debris from its surface. Meanwhile, the left PDMS mixture was poured onto the control-channel mold, degassed, cured for 1 h at 85 °C, and then peeled off from the mold. The surfaces of the two-layer PDMS structure (on the membrane side) and the duplicated control-channel layer were then treated with a hand-held corona treater (BD-20AC, Electro-Technic Products), which ionizes the surrounding air and creates localized plasma to activate the surfaces for irreversible bonding. The intensity of the corona was set at a relatively low level in order to produce a stable but soft corona with minimal crackling and sparking [27]. The wire electrode was positioned approximately 3 mm above the treated surface, and scanned back and forth for 30 s to 1 min, depending on the size of the surface. The corona-treated surfaces were then pressed together and left undisturbed for at least 1 h at 85 °C for the bonding to take effect. At the end, multiple PTFE tubes were inserted into the punched holes to build the necessary interconnection for sample injection and discharge.

Experimental details

In the prototype demonstration, water-in-oil droplets were produced using de-ionized water and oleic acid (Aldrich) with 5 wt% Span 80 (Aldrich) as dispersed and continuous phase fluids, respectively. In addition to oleic acid (viscosity 28 mPa s), hexadecane (viscosity 8 mPa s) and silicone oil (viscosity 50 mPa s) were also tested to investigate the effects caused by the viscosity of continuous-phase fluid. The detailed experimental setup is illustrated in figure 6. An air compressor (Model 3-4, Jun-Air) with its output set at 500 kPa was employed as the single source to drive the operation. Each fluid sample was stored in a separate plastic container, which was fed with pressurized air from the top to drive the fluid flowing through the bottom tube and into the downstream microfluidic devices. The actual driving pressure applied on each container was adjusted independently by a separate pressure regulator (IR1000-01G, SMC). Meanwhile, the actuation of each membrane valve was controlled independently by a separate electromagnetic valve (VK332-5G-M5, SMC), whose action was governed by a computer-controlled relay circuitry. A governing program developed and executed under a software environment (LabVIEW, National Instruments), cooperating with a set of hardware adapter and connector (PCI-6220 + CB-68LP), was employed to coordinate the actuation of the prototype system. As such, the operation can be either pre-programmed or responding to demand in a real-time manner. The formation of liquid-in-liquid droplets was observed under an optical microscope and the images were recorded using a CCD camera also controlled by the computer. The resulting droplets were driven into a 400 μm deep reservoir, where the droplets would be perfect spheres without unwanted deformation. The volumes of the resulting droplets were then estimated based on the observed spherical diameters. For the demonstration of 1 × 8 flow switching, three electromagnetic switches (VK3120-5G-M5, SMC) were utilized to control six sets of membrane valves.

Results and discussion

Prior to the metering and fusion trials, the performance of the membrane valve was characterized with the flow channel empty and open to the atmosphere. With a deformable area of 150 μm (the width of the flow channel) ×150 μm (the width

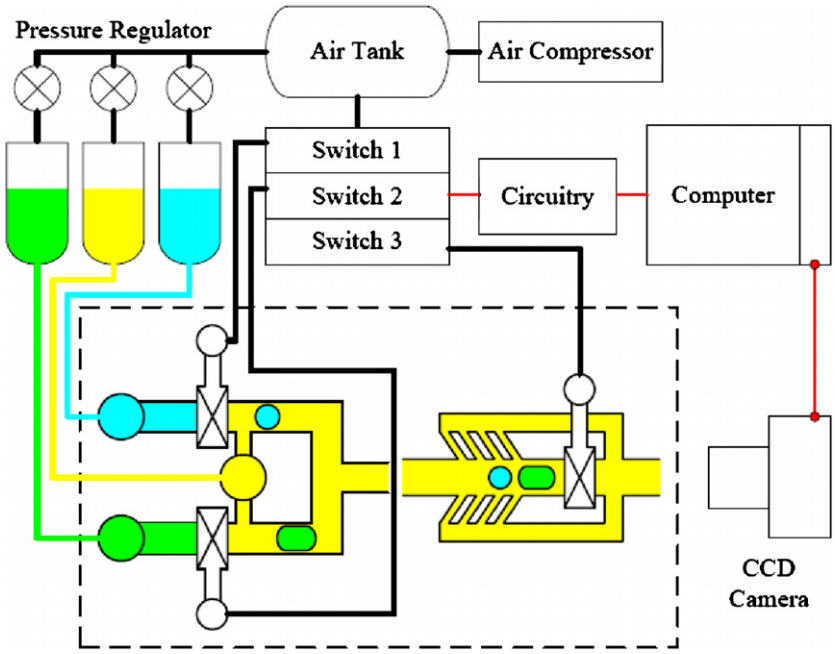

Figure 6. Experimental setup of the proposed droplet metering and fusion schemes.

Table 1. Measured droplet sizes and variations at various valve open time when $P_d = 2.3$ kPa and $P_c = 3.9$ kPa.

Valve open time (s)	0.05	0.1	0.2	0.4	0.8	1.6	2.8
Average droplet diameter (μm)	10.19	17.57	27.16	38.70	51.92	68.36	95.70
Standard variation (%)	3.27	3.72	4.74	1.22	1.49	3.29	1.35
Average droplet volume (pl)	0.55	2.84	10.50	30.34	73.27	167.2	458.8

of the control channel) and a membrane thickness of roughly 30 μm, the minimum pressure required to deflect the membrane and completely block the 25 μm high flow channel was measured to be 75 kPa. At this actuation pressure, the response time of the membrane structure was found to be roughly 0.02 s, which could be further reduced if a higher actuation pressure is employed. The minimum valve open (or close) time actually tested in our experiments was 0.05 s, since the utilized electromagnetic valves were not able to operate correspondingly at frequencies higher than 15 Hz. In the case when the open (or close) time is shorter than the response time of the valve, the valve would only be partially opened (or closed). When working fluids are pressurized and fed into the flow channel, the actual minimum pressure for complete blockage and the resulting response time of the membrane structure would vary accordingly. Usually, fluids with higher viscosities would require higher pressure and longer time for operation.

In the metering trials, the resulting droplet volume (V) was mainly controlled by the valve open time ($T = t_{\text{open}}$) and the driving pressures of the dispersed and continuous phase fluids (P_d and P_c). For steady flow, the volume is expected to be approximately equal to the product of the resulting dispersed-phase flow rate and the valve open time. However, the flow is actually transient right after the valve is opened. The production of a small droplet (with an estimated volume of 11 pL) is illustrated in figure 2. The retreat of the membrane causes a negative pressure gradient, which sucks in the fluids and in turn shapes the front end of the dispersed-phase flow into a cone (as shown in figure 2(c)). Meanwhile, the bulk dispersed-phase fluid is accelerated and starts to flow. After opened for a short period of time, the membrane valve is closed and the dispersed-phase flow is broken, while the volume left to the center line of the membrane is shaped into a droplet. In general, the volume of the resulting droplet would not be linearly proportional to the valve open time, because of the transient effects caused by the retreat of the membrane and the acceleration of the disperse-phase fluid from being blocked. The measured relationship between the resulting droplet volume and the valve open time (with DI water and oleic acid as dispersed and continuous phase fluids, respectively) is illustrated in figure 7. For condition 1 ($P_d =$ 2.3 kPa and $P_c = 3.9$ kPa), the droplet volume fell from 458.8 to 0.55 pL, while the valve open time decreased from 2.8 to 0.05 s. It is found that a 56 times decrease in the valve open time had resulted in a more than 800 times fall in the droplet volume. This nonlinearity is believed to result from the transient effects just mentioned, which are more significant when the valve open time is shorter. Meanwhile, table 1 shows the droplet sizes and variations at various valve open time measured under condition 1. It is noted that the diameter deviation of the resulting droplets is usually less than 5% of the average value, which indicates a desired monodisperse character. When the fluid-driving pressures (P_d and P_c) vary, the relationship between the resulting droplet volume and the valve open time would change as well. Comparatively, when

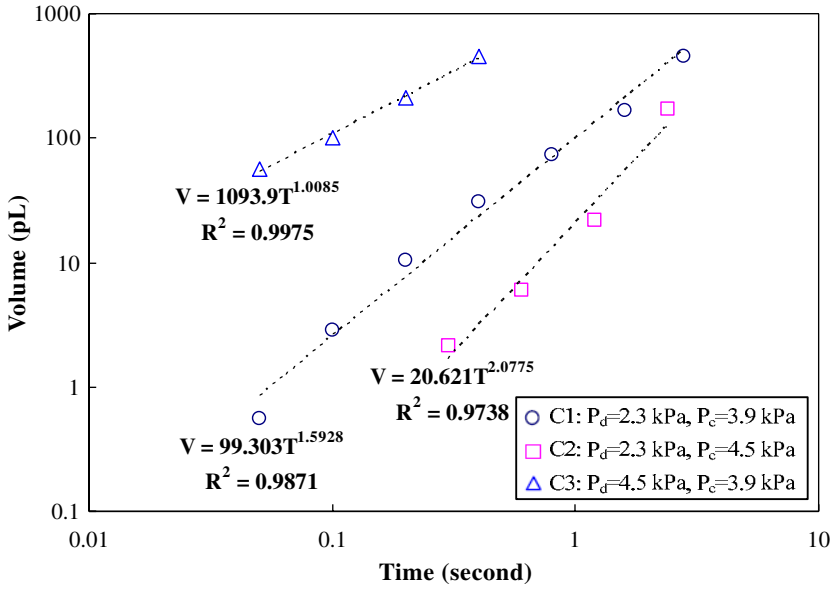

Figure 7. Measured relationship between resulting droplet volume (V) and valve open time (T).

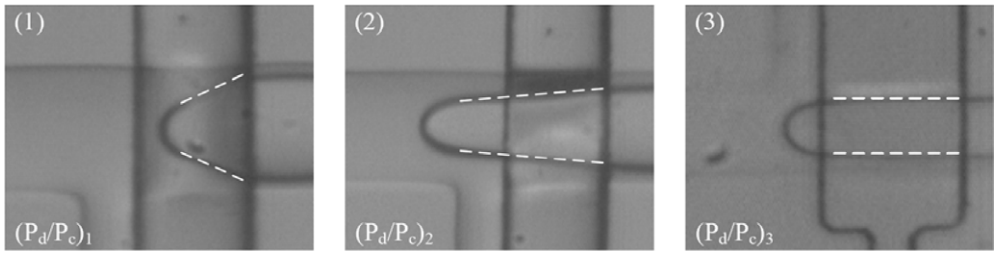

Figure 8. Captured water–oil interfaces with $(P_d/P_c)_3 > (P_d/P_c)_2 > (P_d/P_c)_1$.

Figure 9. Production of a droplet stream with a preset size order of 1×, 2×, 3×, 4×, 3×, 2×, 1×.

P_c was raised from 3.9 to 4.5 kPa (condition 2 in figure 7), the resulting droplet volume became smaller at the same valve open time and plummeted even faster while the valve open time decreased. It is expected that the reduction in the P_d/P_c ratio would lower the resulting dispersed-phase flow rate and amplify the transient effects. Meanwhile, when P_d was raised from 2.3 to 4.5 kPa (condition 3 in figure 7), the relationship between the resulting droplet volume and the valve open time became closer to linear, most likely due to the decline in the transient effects. In general, the relationship between the resulting droplet volume and the valve open time is found to be approximately $V = kT^a$, where k and a are constants determined mainly by the fluid-driving pressures when a specific fluid combination is utilized. For condition 1, constant a is estimated to be 1.59 and k is about 99.30, while (a, k) are (2.08, 20.62) and (1.01, 1094) for conditions 2 and 3, respectively. Meanwhile the employment of a continuous-phase fluid with higher viscosity would usually enhance the transient effects and therefore result in higher nonlinearity and the reduction in dispersed droplet volume. In addition, it is also found that the cone angles of the water–oil interfaces decreased when the corresponding P_d/P_c ratios increased, as shown in figure 8. Based on the measured results, droplets with desired sizes could be produced with negligible delay by the proposed metering scheme. To demonstrate the functionality of this scheme, a LabVIEW program that allows users to assign the individual size and order of the output droplet stream was developed. By adjusting merely the valve open time correspondingly, the production of a droplet stream with a preset size order of 1×, 2×, 3×, 4×, 3×, 2×, 1× was realized as shown in figure 9.

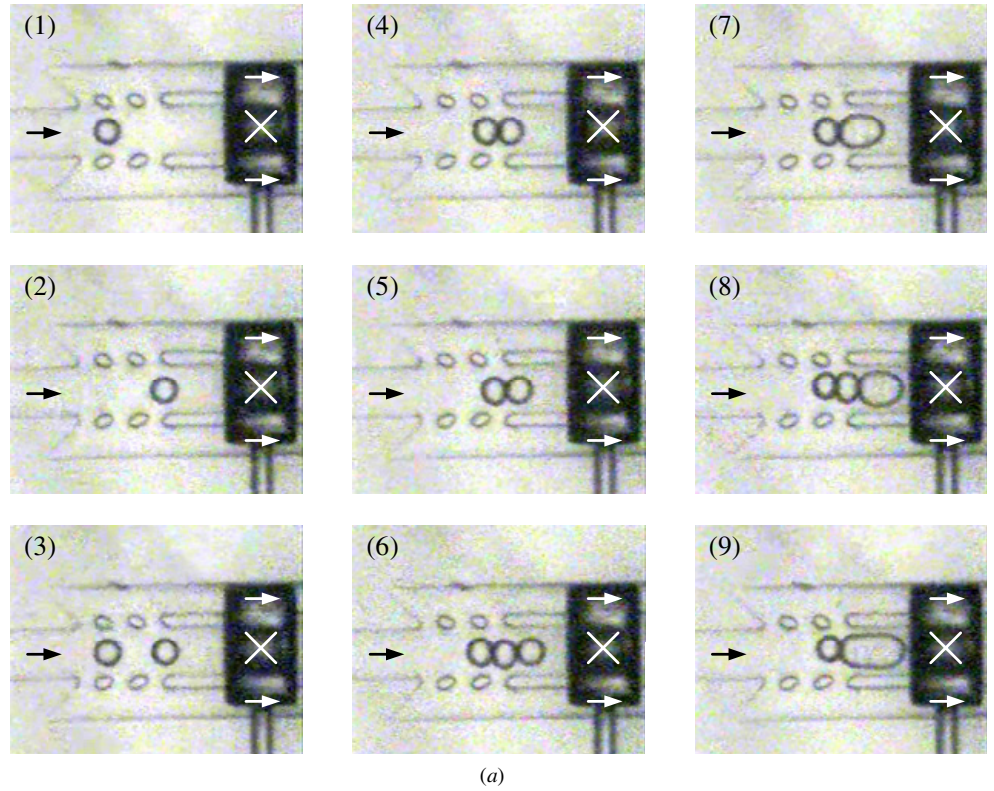

(*a*)

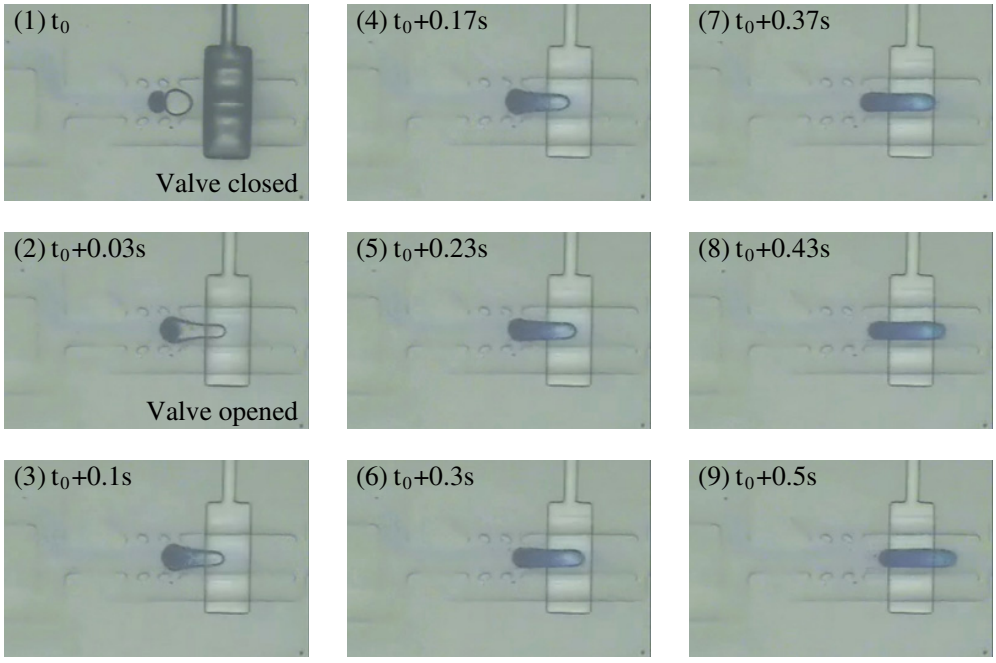

(*b*)

Figure 10. (*a*) Recorded fusion sequences of (*a*) four serially entrapped droplets and (*b*) two entrapped droplets accelerated by the retreat of the membrane.

Figure 10(*a*) shows a recorded fusion sequence, in which the diameters of the incoming droplets were about half of the width of the middle main channel. Although all the three downstream flow channels are intersected by a control channel (valve), only the flow in the main channel would be completely blocked when the valve is activated. The droplet arrived first was entrapped in front of the valve, while the continuous-phase flow bypassed the valve. The following droplets were also driven into the waiting zone, collided and eventually merged with the previously entrapped droplets. If the waiting zone is fully occupied, the incoming droplets would be driven through the bypassing branches and discharged.

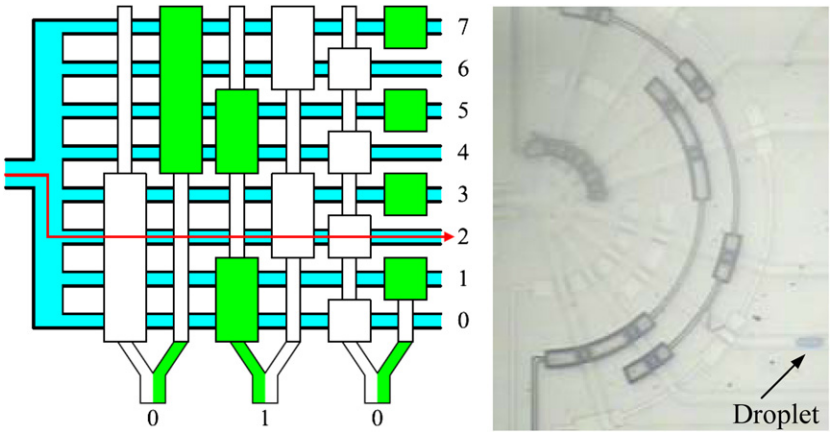

(*a*) (*b*)

Figure 11. Schematic illustration (*a*) and photograph (*b*) of a 1 × 8 flow switch.

The fusion did not happen right after the droplets collided with each other. Instead, the draining of the film between two consecutive droplets would last for a certain period of time, before the two droplets could finally merge together [28]. To shorten the process time, the entrapped droplets were discharged into a diverging channel, in which fusion was accelerated by a decelerating velocity gradient, soon after the collision. Meanwhile, the fusion of the entrapped droplets can also be accelerated by the retreat of the membrane. The retreat causes a negative pressure gradient, which sucks in the fluids and in turn accelerates the draining of the liquid film between the entrapped droplets, as shown in figure 10(*b*). It is observed that the droplets fused together right after (in 0.03 s) the valve was opened and mixed rapidly after the fusion. Compared to other fusion schemes, our approach can handle more droplets and tolerate higher variations in droplet size and the spacing between consecutive droplets. Once all the metering, fusion and mixing steps had been completed, the resulting droplets were selectively delivered into corresponding downstream paths as requested. Figure 11 illustrates a 1 × 8 flow switch [29] that was employed to control the delivery of droplets. Six (=2 × 3) control channels actuated by three external switching valves could result in 8 (=2^3) different delivery paths. For example, an actuation status of 0–1–0, as illustrated in figure 11(*a*), would direct the flow into the No. 2 channel. This concept was implemented and integrated with the metering and fusion devices, as shown in figure 11(*b*). As such, the proposed schemes and the integrated system would be able to produce micro-droplets with desired volumes and compositions, and deliver the resulting droplets into one of the eight destinations upon request.

Conclusion

We have successfully demonstrated an active emulsification scheme that can produce micro-droplets with desired volumes and compositions on demand. Devices with pneumatically actuated membrane valves constructed on top of specially designed microfluidic channels are employed to meter and fuse liquid-in-liquid droplets. By steadily pressurizing a fluid and intermittently blocking its flow, droplets with desired volumes are dispersed into another fluid. Furthermore, droplets from multiple sources are fused together to produce combined droplets with desired compositions. In the prototype demonstration, a three-layer PDMS molding and irreversible bonding process was utilized to fabricate the proposed microfluidic devices. The volume (V) of the dispersed droplets is found to be mainly controlled by the valve open time (T), and the relationship could be approximated as $V = kT^a$, in which k and a are pressure-dependent constants. For a water flow that was driven by a constant-pressure source (at 2.3 kPa) and normally blocked by a membrane valve, the volume of the resulting droplets fell from 458.8 to 0.55 pL (a >800 times drop), while the valve open time decreased from 2.8 to 0.05 s (a merely 56 times reduction). The nonlinearity is believed to result from transient effects, which are more significant when the valve open time is shorter. Meanwhile it is also noted that under the same conditions, the diameter deviation of the resulting droplets was usually less than 5% of the average value, which indicates a desired monodisperse character. In order to produce desired combined droplets and deliver them to intended destinations, functional droplet entrapment, fusion and flow switching devices, which also utilize the membrane valves, were integrated with the metering devices. With four valve control lines, multiple droplets can be entrapped, fused and delivered to one of the eight destinations. As such, the demonstrated microfluidic system could potentially realize the controllability on droplet volume, composition and motion, which is desired for a variety of biological and chemical applications.

Acknowledgments

This work was supported in part by the National Science Council of Taiwan under Contract No. NSC 96-2221-E-007-116-MY3. The demonstrated systems were fabricated in the

ESS Micro-fabrication Lab at National Tsing Hua University, Taiwan.

References

[1] Becher P 1965 *Emulsions: Theory and Practice* (New York: Reinhold)

[2] Lissant K J 1974 *Emulsions and Emulsion Technology* (New York: Dekker)

[3] de Castro M D L and Priego-Capote F 2007 Ultrasound-assisted preparation of liquid samples *Talanta* **72** 321–34

[4] Schultz S, Wagner G, Urban K and Ulrich J 2004 High-pressure homogenization as a process for emulsion formation *Chem. Eng. Technol.* **27** 361–8

[5] Schramm L L 2005 *Emulsions, Foams, and Suspensions: Fundamentals and Applications* (Weinheim: Wiley-VCH)

[6] Benita S 1996 *Microencapsulation: Methods and Industrial Application* (New York: Dekker)

[7] Thorsen T, Roberts R W, Arnold F H and Quake S R 2001 Dynamic pattern formation in a vesicle-generating microfluidic device *Phys. Rev. Lett.* **86** 4163–6

[8] Nisisako T, Torii T and Higuchi T 2002 Droplet formation in a microchannel network *Lab Chip* **2** 24–6

[9] Dendukuri D, Tsoi K, Hatton T A and Doyle P S 2005 Controlled synthesis of nonspherical microparticles using microfluidics *Langmuir* **21** 2113–6

[10] Anna S L, Bontoux N and Stone H A 2003 Formation of dispersions using "flow focusing" in microchannels *Appl. Phys. Lett.* **82** 364–6

[11] Garstecki P, Gitlin I, DiLuzio W and Whiteside G M 2004 Formation of monodisperse bubbles in a microfluidic flow-focusing device *Appl. Phys. Lett.* **85** 2649–51

[12] Tan Y C, Fisher J S, Lee A I, Cristini V and Lee A P 2004 Design of microfluidic channel geometries for the control of droplet volume, chemical concentration, and sorting *Lab Chip* **4** 292–8

[13] Song H, Chen D L and Ismagilov R F 2006 Reactions in droplets in microfluidic channels *Angew. Chem. Int. Edit.* **45** 7336–56

[14] Kelly B T, Baret J C, Taly V and Griffiths D 2007 Miniaturizing chemistry and biology in microdroplets *Chem. Commun.* **18** 1773–88

[15] Leamon J H, Link D R, Egholm M and Rothberg J M 2006 Overview: methods and applications for droplet compartmentalization of biology *Nat. Methods* **3** 541–3

[16] Zheng B, Roach L S and Ismagilov R F 2003 Screening of protein crystallization conditions on a microfluidic chip using nanoliter-size droplets *J. Am. Chem. Soc.* **125** 11170–1

[17] Martin K, Henkel T, Baier V, Grodrian A, Schon T, Roth M, Kohler J M and Metze J 2003 Generation of larger numbers of separated microbial populations by cultivation in segmented-flow microdevices *Lab Chip* **3** 202–7

[18] Khan S A, Gunther A, Schmidt M A and Jensen K F 2004 Microfluidic synthesis of colloidal silica *Langmuir* **20** 8604–11

[19] Dittrich P S and Manz A 2006 Lab-on-a-chip: microfluidics in drug discovery *Nat. Rev. Drug Discovery* **5** 210–8

[20] Joanicot M and Ajdari A 2005 Droplet control for microfluidics *Science* **309** 887–8

[21] Christopher G F and Anna S L 2007 Microfluidic methods for generating continuous droplet streams *J. Phys. D Appl. Phys.* **40** R319–36

[22] Song H, Tice J D and Ismagilov R F 2003 A microfluidic system for controlling reaction networks in time *Angew. Chem. Int. Edit.* **42** 768–72

[23] Hung L H, Choi K M, Tseng W Y, Tan Y C, Shea K J and Lee A P 2006 Alternating droplet generation and controlled dynamic droplet fusion in microfluidic device for CdS nanoparticle synthesis *Lab Chip* **6** 174–8

[24] Link D R, Grasland-Mongrain E, Duri A, Sarrazin F, Cheng Z, Cristobal G, Marquez M and Weitz D A 2006 Electric control of droplets in microfluidic devices *Angew. Chem. Int. Edit.* **45** 2556–60

[25] Unger M A, Chou H P, Thorsen T, Scherer A and Quake S R 2000 Monolithic microfabricated valves and pumps by multilayer soft lithography *Science* **288** 113–6

[26] Duffy D C, McDonald J C, Schueller O J A and Whitesides G M 1998 Rapid prototyping of microfluidic systems in poly(dimethylsiloxane) *Anal. Chem.* **70** 4974–84

[27] Haubert K, Drier T and Beebe D 2006 PDMS bonding by means of a portable, low-cost corona system *Lab Chip* **6** 1548–9

[28] Chesters A K 1991 The modelling of coalescence processes in fluid-liquid dispersions: a review of current understanding *Trans. Inst. Chem. Eng.* A **69** 259–70

[29] Thorsen T, Maerkl S J and Quake S R 2002 Microfluidic large-scale integration *Science* **298** 580–4